Pre-Report
2DA1201Y PNP TRANSISTOR

Adrija Bera 210071

Pratyush Amrit 210762

Devendra Kumar Saini 241040608

Aniket Sen 210134

Abstract

Analysis and extraction of model parameters and performance characterization of 2DA1201Y PNP transistor.

1 Theoretical Expressions

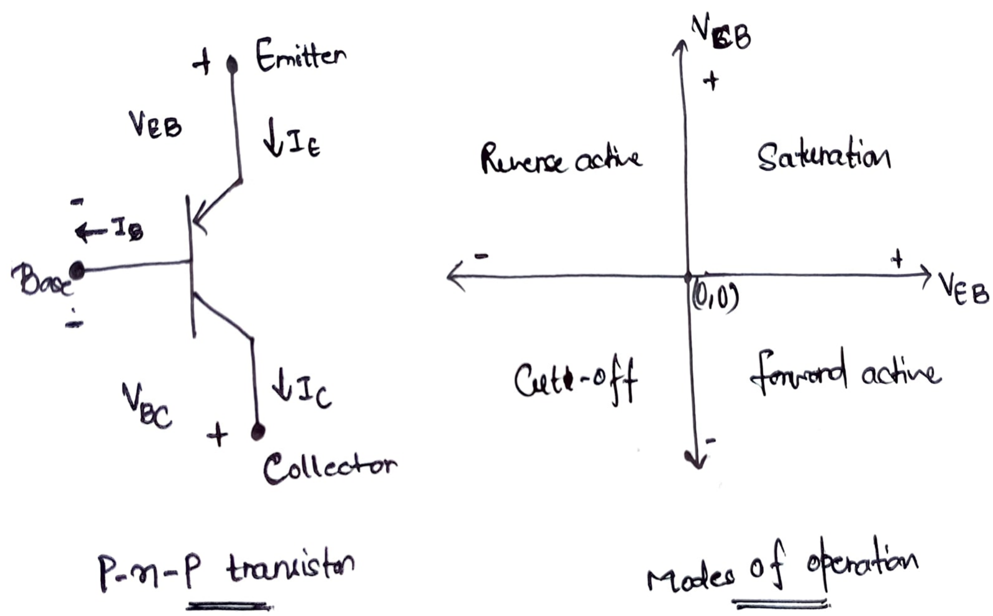

Figure 1: Structure of PNP BJT

For the P-N-P transistor, as shown in Figure 2, we have:

- N_{AE} = Doping concentration of acceptor atoms in the emitter region.
- N_{DB} = Doping concentration of donor atoms in the base region.
- N_{AC} = Doping concentration of acceptor atoms in the collector region.

In the forward active mode of operation of the P-N-P BJT, when $V_{EB} > 0$ and $V_{CB} < 0$, we will have the injection of electrons into the emitter from the base and holes into the base from the emitter. The electron concentration at the emitter-base depletion layer surface is given by:

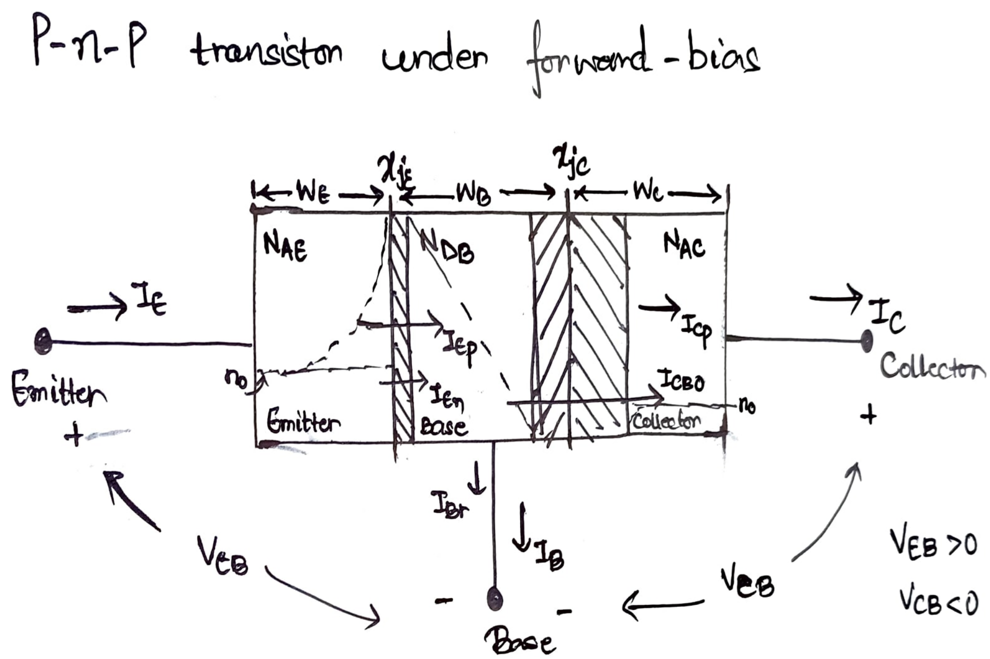

Figure 2: Working of PNP BJT in forward active mode

- n_p = Concentration of Electrons injected from the base into the emitter at the depletion layer surface.

$$n_p = n_{po} \exp\left(\frac{V_{EB}}{V_t}\right); n_{po} = \frac{{n_i}^2}{N_{AE}} \tag{1}$$

where V_t is the thermal voltage & n_i is the intrinsic concentration of Carrier at given temperature for all expression.Therefore, Excess Electron concentration at Depletion layer surface after injection on emitter side is given by,

$$\Delta n_p = n_p - n_{po} = n_{po}[\exp\left(\frac{V_{EB}}{V_t}\right) - 1] \tag{2}$$

- p_n = Concentration of Holes injected from the emitter into the base at the depletion layer surface.

$$p_n = p_{no} \exp\left(\frac{V_{EB}}{V_t}\right); p_{no} = \frac{{n_i}^2}{N_{DB}} \tag{3}$$

Since, The Collector-Base junction is under Reverse bias is under reverse bias, due to carrier extraction at surface the hole concentration at surface on base side is given by,

$$p_{nCB} = p_{no} \exp\left(\frac{V_{CB}}{V_t}\right); V_{CB} < 0 \Rightarrow p_{nCB} \approx 0 \tag{4}$$

The base width (W_E) of the transistor is kept much smaller than the diffusion length (L_p) of the holes, So that all the holes injected from emitter side travels through the base region with minimum injection resulting in a Collector current much greater than reverse saturation current of Base-Collector such that, $I_C \approx I_E$.

We can define 5 main components of current in BJT as shown in figure 2.

- I_{Ep} = Current due to hole injection on Base side from Emitter.
- I_{En} = Current due to Electron injection on Emitter side from Base.
- I_{Br} = Current due to recombination of holes in base region.
- I_{Cp} = Current due to Collection of holes from base region.
- I_{CBO} = Reverse saturation current across Base-Collector.

2 Current Components and Device Parameters

2.1 Emitter Current (I_E)

The total emitter current is composed of two components: the hole current injected from the emitter into the base (I_{Ep}) and the electron current injected from the base into the emitter (I_{En}). Thus, the emitter current is:

$$I_E = I_{Ep} + I_{En} \tag{5}$$

The diffusion current is given by Fick's first law of diffusion:

$$J_p(x) = -qD_p \frac{dp_n(x)}{dx} \tag{6}$$

where $J_p(x)$ is the hole current density at a distance x into the base, D_p is the diffusion coefficient of holes, and $p_n(x)$ is the hole concentration at distance x from the depletion surface. for cross-sectional area A,

$$I_{Ep} = J_p(0)A = qAD_p \left.\frac{dp_n(x)}{dx}\right|_{x=0} \tag{7}$$

From current-continuity equation in steady-state conditions,

$$\frac{d^2\Delta p_n(x)}{dx^2} = \frac{\Delta p_n(x)}{L_p^2} \tag{8}$$

where L_p is the diffusion length of holes in the base. The solution to this differential equation for a uniform base width W_B and boundary conditions at the base-emitter and base-collector junctions is:

$$\Delta p_n(x) = \Delta p_{no} \exp\left(\frac{-x}{L_p}\right); \Delta p_{no} = \frac{{n_i}^2}{N_{DB}}[\exp\left(\frac{V_{EB}}{V_t}\right) - 1] \tag{9}$$

$$\Delta p_n(0) = \Delta p_{no} = \frac{{n_i}^2}{N_{DB}}[\exp\left(\frac{V_{EB}}{V_t}\right) - 1] \tag{10}$$

Simplification for $W_B \ll L_p$ from Taylor's expansion,

$$\Delta p_n(x) = \Delta p_{no}[1 - \frac{x}{W_B}] \tag{11}$$

$$\Rightarrow I_{Ep} = qAD_p \frac{\Delta p_n(0)}{W_B} = \frac{qAD_p{n_i}^2}{N_{DB}W_B}[\exp\left(\frac{V_{EB}}{V_t}\right) - 1] \tag{12}$$

$$I_{Ep} \approx \frac{qAD_p{n_i}^2}{N_{DB}W_B} \exp\left(\frac{V_{EB}}{V_t}\right) \tag{13}$$

Similarly I_{En} can be found as,

1. For short length Emitter i.e Emitter thickness W_E « electron diffusion length on emitter side L_n,

$$I_{En} \approx \frac{qAD_n{n_i}^2}{N_{AE}W_E} \exp\left(\frac{V_{EB}}{V_t}\right) \tag{14}$$

2. for Long length Emitter

$$I_{En} \approx \frac{qAD_n {n_i}^2}{N_{AE}L_n} \exp\left(\frac{V_{EB}}{V_t}\right) \tag{15}$$

Final Expression for Emitter Current, I_E = $I_{Ep} + I_{En}$

$$I_E = \frac{qAD_n {n_i}^2}{N_{AE}W_E} \exp\left(\frac{V_{EB}}{V_t}\right) + \frac{qAD_p {n_i}^2}{N_{AE}L_n} \exp\left(\frac{V_{EB}}{V_t}\right)$$

Since $N_{AE} >> N_{DB} \Rightarrow I_E \approx I_{Ep}$ hence,

$$\boxed{I_E \approx I_{Ep} \approx \frac{qAD_p {n_i}^2}{N_{DB}W_B} \exp\left(\frac{V_{EB}}{V_t}\right)} \tag{16}$$

2.2 Base Current (I_B)

The base current is the sum of the current due to recombination of holes in the base region (I_{Br}) and the electron current injected into the emitter from the base minus the collector current:

$$I_B = I_{Br} + I_{En} - I_{CBO} \tag{17}$$

Base current can be found from the charge control model:

$$I_B = \frac{Q_p}{\tau_p} = \frac{qAW_B p_n}{2\tau_p} = \frac{qAW_B p_{n0}}{2\tau_p} \exp\left(\frac{V_{EB}}{V_T}\right)$$

$$\boxed{I_B = \frac{qAW_B {n_i}^2}{2N_{DB}\tau_p} \exp\left(\frac{V_{EB}}{V_T}\right)} \tag{18}$$

2.3 Collector Current (I_C)

The collector current is due to the collection of holes injected into the base and reverse saturation current which is very small.

$$I_C = I_{cp} + I_{CBO}$$

$$I_C \approx I_{cp} \tag{19}$$

2.4 Base Transport Factor (B)

The base transport factor α_T is defined as the fraction of holes injected into the base that reach the collector without recombining.

$$B = \frac{I_{Cp}}{I_{Ep}} = \frac{I_{Ep} - I_B}{I_{Ep}} = 1 - \frac{I_B}{I_{Ep}}$$

$$B = 1 - \frac{{W_B}^2}{2{L_p}^2}, ({L_p}^2 = D_P\tau_p) \tag{20}$$

where W_B is the base width and L_p is the diffusion length of holes in the base.

2.5 Emitter Efficiency (γ)

The emitter efficiency γ is defined as the ratio of the hole current injected into the base to the total emitter current:

$$\gamma = \frac{I_{Ep}}{I_E} = \frac{I_{Ep}}{I_{Ep} + I_{En}} = \left[1 + \frac{I_{En}}{I_{Ep}}\right]^{-1}$$

$$\gamma = \left[1 + \frac{D_n W_B N_{DB}}{D_P L_p N_{AE}}\right]^{-1} \text{(long emitter)} \tag{21}$$

$$\gamma = \left[1 + \frac{D_n W_B N_{DB}}{D_P W_E N_{AE}}\right]^{-1} \text{(short emitter)} \tag{22}$$

2.6 Current Gain (α_f and β)

The current gain α_f is the ratio of the collector current to the emitter current:

$$\alpha_f = \frac{I_C}{I_E} \approx \frac{I_{Cp}}{I_{Ep} + I_{En}} = B\gamma \tag{23}$$

The common-emitter current gain β_f is the ratio of the collector current to the base current:

$$\beta_f = \frac{I_C}{I_B} = \frac{I_C}{I_E - I_C} = \frac{\alpha_f}{1 - \alpha_f} \tag{24}$$

2.7 Switching Characteristics

$$\tau_f = \frac{{W_B}^2}{2D_p} \tag{25}$$

3 Information extraction from plots

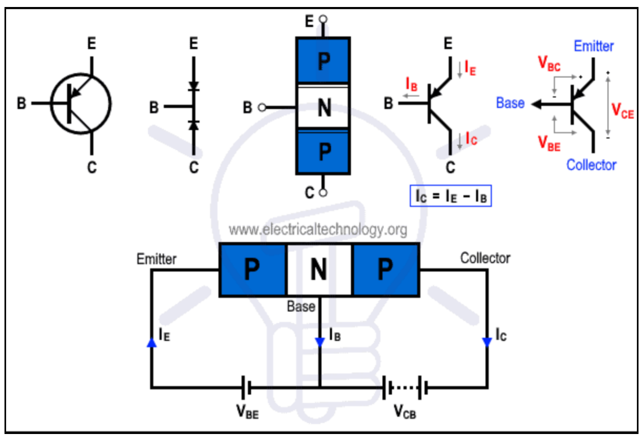

Figure 3: Construction and working of PNP BJT

Power limit variation with temperature

- The relation with P$_tot$

- **Inversion** : Images are inverted so that the background black matches with extra black pixels introduced around the corners due to rotation.
- **Erosion** : This is used to reduce the thickness of lines present in the image. As a result, the obstructing lines are almost removed. The thickness of letters also got reduced but they are still good enough to be further used.
- **Rotation** : 7 copies of each reference character are made with rotation angles of $-30, -20, -10, 0, 10, 20, 30$ degrees and stored as new reference images in an array. These are used for comparison on the training/testing images.

Step 2: Cropping and Comparison with Reference Set

- **Cropping** : Obtained test image is cropped using a manually tuned parameter in order to extract last character.
- Dimensionality of images are made consistent through appropriate cropping of reference images.
- Each image is then compared with each of 16×7 reference images through the process of **'Subtraction'**.

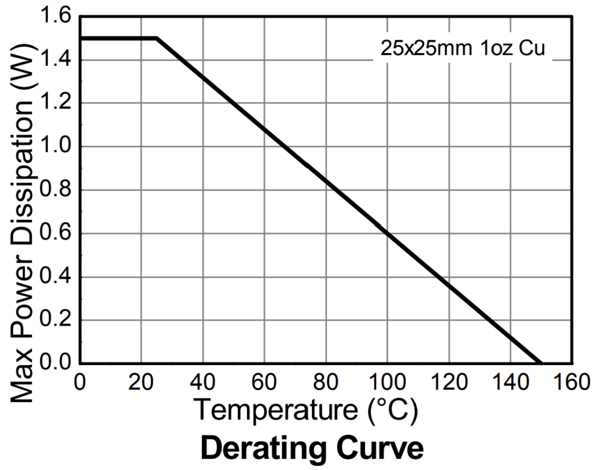

Figure 4: Derating curve

Step 3: Correct classification based on Subtraction matrix

- Each test image is compared with 16×7 reference images and sum of elements of difference matrix(D) is stored in a new matrix.
- Least element of the new matrix gives us the most resembled character and the algorithm outputs the same.

Step 4: Parity detection

After successful identification of last character, parity of the last character is found by using the modulo operator which gives us the parity of the hexadecimal number itself.

4 Hyper-Parameter Tuning

"Selecting an optimal value for a hyper-parameter is often considered an art rather than a science."

Hence, there exists no fixed algorithm to find out the best hyper-parameters. Instead, it depends on its utility in the Machine Learning model .

The hyper-parameters used in our attempt are as follows:

1. Monochrome Threshold
2. Eroding Thickness
3. Cropping Last Character
4. Horizontal Cropping of Reference Images
5. Vertical Cropping of Reference Images
6. Resizing Parameter

4.1 MonochromeThreshold

Firstly, the images are converted to gray-scale to remove the unnecessary information of colors. Then, the images are converted to monochrome using a thresholding parameter, which is determined using the *Otsu's Method*.

4.2 Eroding Thickness

The erosion parameter is the kernel size. Kernel is the structuring element that determines the precise effect of the erosion on the input image. A too low size would not affect at all while a too large kernel size erodes the boundaries of the characters too. A kernel size of 2 gave optimum results as to eroding obstructing lines as well as maintaining legible thickness of characters in image.

4.3 Cropping Last Character

For obtaining the last character which is crucial to parity generation, we crop the test image with a boundary of $10 : 100 \times 360 : 450$ pixels. This was found manually. We used matplotlib.pyplot to display the image in an XY plot. We found the right X and Y axes limits which bounded a straight image closely, $378 : 432$ and $18 : 92$ respectively(refer Fig.1). Then, cropped it with an offset of 18 horizontally on both sides and an offset of 8 vertically above and below so that the boundary could hold the character even if it was rotated to ± 30 degrees (refer Fig.2). This results in a 90×90 image, with boundaries $10 : 100 \times 360 : 450$ pixels.

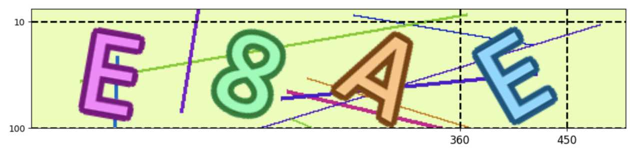

Figure 5: Boundary chosen to Enclose $\pm 30°$ Rotated ones

4.4 Horizontal Cropping of Reference Images

First limitation is that the reference image should also be 90×90 for subtraction. We cropped the image instead of resizing it from 100×100 to 90×90, so that the resolution of image doesn't change. The possible horizontal cropping limits are from $0 : 90$ to $10 : 100$. We have tuned this as a hyper-parameter and found that $5 : 95$ gave 100% accuracy in parity detection.

4.5 Vertical Cropping of Reference Images

The possible vertical cropping limits are from $0 : 90$ to $10 : 100$. We have tuned this as a hyper-parameter and found that $3 : 93$ gave 100% accuracy in parity detection.

4.6 Resizing Parameter

We resized both test and reference images to the same values after cropping them both to 90×90 matrices. We tried to resize the images initially, to a smaller value say, 50×50 pixels, to reduce computing time and found a significant drop in accuracy. So, we tried tuning it as a hyper-parameter.

The below heat maps show the Parity Accuracy w.r.t to the resizing hyper-parameter and different cropping hyper-parameters of the reference images. So, from Fig.3(c),(d),(e), we chose the best horizontal crop as $5 : 95$. From Fig.3(d), we chose the best vertical crop as $3 : 93$ and the resizing limit as 87×87 pixels.

Hyper-Parameter Tuning

5 Conclusion

Based on the above images and fine-tuning of various hyper-parameters, we have reached the following conclusions:

- Using pictures in gray-scale and turning them into monochrome resulted in better identification and reduced the execution time around $3 - 4$ milliseconds.

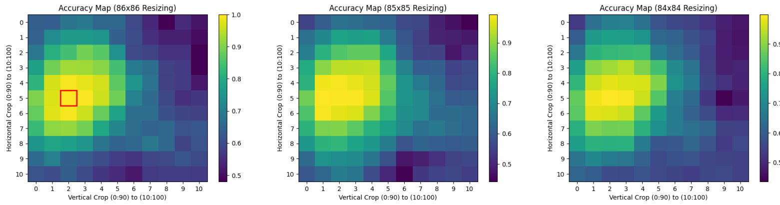

(a) 86×86 pixels (b) 85×85 pixels (c) 84×84 pixels

Figure 6: X axis and Y axis represent the vertical crop offset and the horizontal crop offset of the reference images respectively. The red blocks show 100% accuracy in parity detection.

- Optimized sizes of respective images were found through manually looking at the training image and fine-tuning the hyper-parameters for reference images.
- Subtraction method provided an appreciable parity accuracy.

Through the optimization process outlined above, our model achieved a **parity match score of** 1.0 (accuracy of 100%) within an execution time of 7 **milliseconds** per image when 2000 images were used. (subject to change because the first iteration takes around 60 milliseconds due to reference image pre-processing).

References

[1] OpenCV Tutorial for Erosion and Image Morphology

[2] Documentation for *Otsu's method*

[3]Algorithm for Subtraction of Image Matrix